

# Experimental evidence for diel variations of the carbon isotope composition in leaf, stem and phloem sap organic matter in *Ricinus communis*

ARTHUR GESSLER<sup>1\*†</sup>, GUILLAUME TCHERKEZ<sup>1,3\*</sup>, ANDREAS D. PEUKE<sup>2</sup>, JALEH GHASHGHAIE<sup>3</sup> & GRAHAM D. FARQUHAR<sup>1</sup>

<sup>1</sup>Environmental Biology Group, Research School of Biological Sciences, Australian National University, GPO Box 475, Canberra, ACT 2601, Australia, <sup>2</sup>School of Biological, Earth and Environmental Sciences, University of New South Wales, Sydney, New South Wales 2052, Australia and <sup>3</sup>Laboratoire d'Ecologie, Systématique et Evolution, Département d'Ecophysiologie Végétale, CNRS-UMR 8079, IFR 87, Centre scientifique d'Orsay, Bâtiment 362, Université Paris-Sud XI, 91405 Orsay, Cedex, France

## ABSTRACT

Carbon isotope fractionation in metabolic processes following carboxylation of ribulose-1,5-bisphosphate (RuBP) is not as well described as the discrimination during photosynthetic CO<sub>2</sub> fixation. However, post-carboxylation fractionation can influence the diel variation of  $\delta^{13}\text{C}$  of leaf-exported organic matter and can cause inter-organ differences in  $\delta^{13}\text{C}$ . To obtain a more mechanistic understanding of post-carboxylation modification of the isotopic signal as governed by physiological and environmental controls, we combined the modelling approach of Tcherkez *et al.*, which describes the isotopic fractionation in primary metabolism with the experimental determination of  $\delta^{13}\text{C}$  in leaf and phloem sap and root carbon pools during a full diel course. There was a strong diel variation of leaf water-soluble organic matter and phloem sap sugars with relatively <sup>13</sup>C depleted carbon produced and exported during the day and enriched carbon during the night. The isotopic modelling approach reproduces the experimentally determined day–night differences in  $\delta^{13}\text{C}$  of leaf-exported carbon in *Ricinus communis*. These findings support the idea that patterns of transitory starch accumulation and remobilization govern the diel rhythm of  $\delta^{13}\text{C}$  in organic matter exported by leaves. Integrated over the whole 24 h day, leaf-exported carbon was enriched in <sup>13</sup>C as compared with the primary assimilates. This may contribute to the well-known – yet poorly explained – relative <sup>13</sup>C depletion of autotrophic organs compared with other plant parts. We thus emphasize the need to consider post-carboxylation fractionations for studies that use  $\delta^{13}\text{C}$  for assessing environmental effects like water availability on ratio of mole fractions of CO<sub>2</sub> inside and outside the leaf (e.g. tree ring

studies), or for partitioning of CO<sub>2</sub> fluxes at the ecosystem level.

*Key-words:* isotope modelling; post-carboxylation fractionation; starch; transport.

## INTRODUCTION

Whereas carbon isotope discrimination during photosynthetic CO<sub>2</sub> fixation is a comparatively well-described and understood phenomenon (Farquhar, O'Leary & Berry 1982; Farquhar, Ehleringer & Hubick 1989), much less is known about the isotopic fractionation associated with the metabolic processes following carboxylation in leaf tissues (Hobbie & Werner 2004; Badeck *et al.* 2005; Brandes *et al.* 2006). However, fractionations because of equilibrium, kinetic and fragmentation (Tcherkez *et al.* 2004) isotope effects beyond CO<sub>2</sub> diffusion and fixation by ribulose 1·5-bisphosphate carboxylase/oxygenase (Rubisco) are of importance because they result in differences in isotopic signatures among metabolites and in non-statistical intramolecular isotope distributions (Schmidt & Gleixner 1998; Schmidt 2003; Tcherkez & Farquhar 2005).

Among the most obvious consequences of these effects is that the carbon isotope composition of organic matter may differ between plant organs depending on the  $\delta^{13}\text{C}$  of exported and non-exported compounds. Badeck *et al.* (2005) reviewed more than 80 publications for differences in  $\delta^{13}\text{C}$  between organs and showed that heterotrophic tissues are generally enriched in <sup>13</sup>C compared with autotrophic organs. As temporal variations in photosynthetic discrimination were excluded as an explanation of inter-organ differences, there must be either post-carboxylation fractionation in autotrophic tissues and export of <sup>13</sup>C-enriched metabolites across organ boundaries (Hobbie & Werner 2004) or fractionation during heterotrophic metabolism (Helle & Schleser 2004), or both (Brandes *et al.* 2006).

Post-carboxylation carbon isotope fractionation might account for diel variations in the isotopic composition of carbon exported from the leaves to heterotrophic tissues

Correspondence: A. Gessler. Fax: +497612038302; e-mail: arthur.gessler@sonne.uni-freiburg.de

\*Both authors contributed equally to this paper.

†Present address: Core Facility Metabolomics, Centre for Systems Biology, University of Freiburg, 79100 Freiburg, Germany.

(Tcherkez *et al.* 2004; Brandes *et al.* 2006). Transitory starch, the origin of phloem-loaded sugars during the night, can carry  $\delta^{13}\text{C}$  signatures up to about 4‰ greater than triose-P originating directly from the Calvin–Benson cycle (Gleixner *et al.* 1998).

The occurrence of diel variations and intra-plant gradients in  $\delta^{13}\text{C}$  of organic matter are directly relevant to approaches that use the isotopic signature of  $\text{CO}_2$  exchange fluxes at the ecosystem level for the reconstruction of individual sinks and sources (Yakir & Wang 1996; Bowling, Tans & Monson 2001; Pataki *et al.* 2003; Badeck *et al.* 2005) as the isotopic signature of the organic substrate for respiration is imprinted on the respired  $\text{CO}_2$  (Barbour *et al.* 2005; Knohl *et al.* 2005). In addition, the interpretation of  $\delta^{13}\text{C}$  in different plant materials as a time-integrating proxy for environmental effects on ratio of mole fractions of  $\text{CO}_2$  inside and outside the leaf ( $c_i/c_a$ ) may be complicated by post-carboxylation changes of  $\delta^{13}\text{C}$  (Gessler, Rennenberg & Keitel 2004; Helle & Schleser 2004).

At the leaf level, the impact of post-carboxylation isotope effects has been assessed using the modelling approach of Tcherkez *et al.* (2004). Those authors examined the origin of the non-statistical intramolecular distribution of  $^{13}\text{C}$  in hexoses by relating it to the reactions of plant primary carbon metabolism. The model takes into account C–C bond-breaking reactions of the Calvin cycle and gives a mathematical expression for the isotope ratios in hexoses in the steady state. While the estimated fractionations associated with transketolase and aldolase enzymes are sensitive to the flux of starch synthesis parameterized in the model, it is unequivocally predicted that a day–night difference in carbon isotopic composition of leaf-exported carbon should occur, with a  $^{13}\text{C}$  enrichment in the dark period when starch is decomposed to give dark sucrose and a  $^{13}\text{C}$  depletion in the light because of the use of  $^{12}\text{C}$ -enriched triose phosphates from the chloroplast to produce day sucrose. If true, this prediction would be significant, because it would contribute to explaining the isotopic differences between organs outlined earlier. However, until now, there has been no direct experimental evidence showing such a diurnal oscillation of the  $\delta^{13}\text{C}$  of exported carbon.

In the present study, we therefore tested the  $^{13}\text{C}$ -cyclicality prediction of Tcherkez *et al.* (2004) by analysing  $\delta^{13}\text{C}$  in different organic matter pools in leaves (non-exportable, exportable), stems (total organic matter and phloem sap organic matter) and roots (total organic matter) during a light–dark cycle in greenhouse-grown *Ricinus communis* plants. To further assess the cause of inter-organ differences in carbon isotope composition, we compared the  $\delta^{13}\text{C}$  of primary assimilates with the exportable and the non-exportable carbon from the leaves and with phloem sap organic matter transported along the stem axis to the roots. In addition, we combined the modelling of isotopic fractionation in primary metabolism with the experimental determination of  $\delta^{13}\text{C}$  in different plant carbon pools. An agreement between measured and predicted values has been observed, showing indeed that post-carboxylation fractionations have occurred and correlated with the  $\delta^{13}\text{C}$  circadian rhythm. Our

findings may have pervasive implications, namely, for photosynthetic isotope discrimination models that aim to explain the  $\delta^{13}\text{C}$  value of plant organic matter.

## MATERIALS AND METHODS

### Plant material

Seeds of *Ricinus communis* L. were germinated in vermiculite moistened with 0.5 mM  $\text{CaSO}_4$ . After 13–15 d, the plants were transferred to 5 L pots with substrate consisting of commercial potting soil (two parts) (Floradur; Floragard GmbH, Oldenburg Germany) and Perlite (one part) (Perligran; G, Deutsche Perlite GmbH, Dortmund, Germany). Every third day, the pots were irrigated with tap water, and after 1 month on substrate, the plants were supplied with a commercial fertilizer (0.3% Hakaphos Blau; Compo GmbH, Münster, Germany).

The plants were cultivated for 35–40 d in a greenhouse ( $26 \pm 5^\circ\text{C}$ ) with a 16 h photoperiod provided by natural daylight plus mercury-vapour lamps (Osram HQL 400; Osram, Munich, Germany) supplying the plant with a minimum of 300–500  $\mu\text{mol photons m}^{-2} \text{s}^{-1}$ .

### Experimental design

The  $\delta^{13}\text{C}$  of phloem sap-transported organic matter was determined at six different positions (a–f, Fig. 1) along the axis at six time points {four in the light [1030, 1200, 1630, 1900 h ( $\pm$  approx. 1 h)] and two in the dark period [2400, 0300 h ( $\pm$  approx. 1 h)]} during a diel course according to Gessler *et al.* (2007a). At each time point, three to four plants were harvested. Phloem sap was sampled by cutting the bark with a scalpel as described by Jeschke & Pate (1991). After sampling of the phloem sap, stem sections with a length of ca. 3 cm were collected from the same positions. In addition, all seven fully expanded leaves (L1–L7) and fine roots (diameter < 2 mm) were harvested at each time point for the analysis of carbon isotope composition and carbon content in total bulk, water-soluble organic matter (WSOM) and water-insoluble organic matter (IOM) (Fig. 1).

### Extraction of different carbon compounds

All tissue samples (leaves, stem sections and roots) were homogenized in liquid nitrogen. For the extraction of WSOM and IOM, 1.5 mL of deionized water was added to 0.1 g aliquots of freshly frozen plant material. The mixture was agitated for 1 h at  $4^\circ\text{C}$ , and then the extract was boiled at  $100^\circ\text{C}$  for 1 min to precipitate proteins and was centrifuged (12 000 g for 5 min at  $4^\circ\text{C}$ ). The supernatant was considered to be the water-soluble (exportable) fraction consisting mainly of sugars but with some amino acids and organic acids, and the pellet to be the water-insoluble (non-exportable) fraction (Brandes *et al.* 2006).

$\delta^{13}\text{C}$  in starch extracts was analysed in leaves L7, L5, L4 and L3 harvested at 1600 h and 0300 h. Determination of

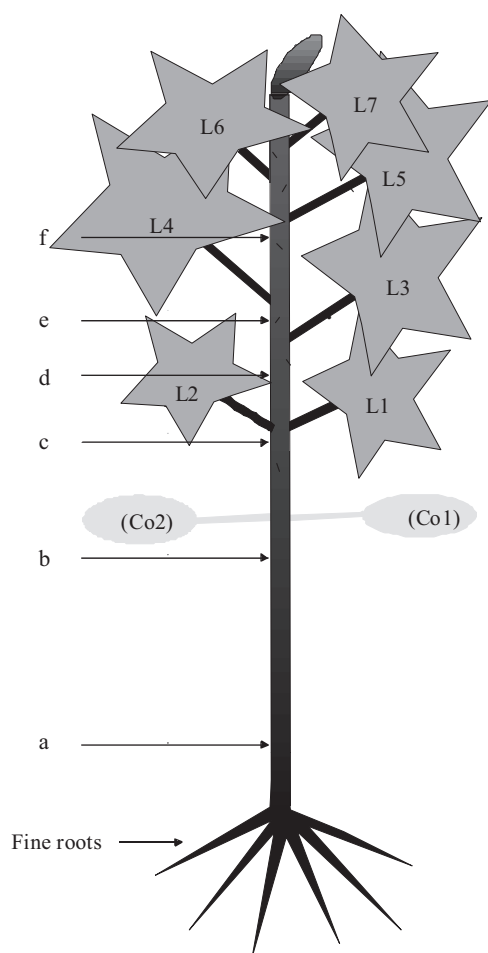


**Figure 1.** Scheme of the plants used in the experiments with sampling positions. For the analysis of phloem sap organic matter, phloem sap was obtained from six positions along the stem (a–f) at six time points during a diel course. From the same position, stem sections were harvested after phloem sampling. The cotyledons (Co1 and Co2) were already dropped at the start of the experiments. Net  $\text{CO}_2$  exchange, ratio of mole fractions of  $\text{CO}_2$  inside and outside the leaf and carbon isotope composition were determined for all fully developed leaves (L1–L7) at the six time points before they were harvested. In addition, at all time points, fine root samples were collected. Mean plant height was 0.65 m.

$\delta^{13}\text{C}$  in starch was performed by modifying the method described by Wanek, Heintel & Richter (2001) and Göttlicher *et al.* (2006). One hundred milligrams of oven-dried leaves were incubated at  $70^\circ\text{C}$  for 30 min in 1.5 mL of a methanol/chloroform/water solution (12:5:3 v : v : v) to completely remove soluble carbohydrates. This step was repeated three times, and the samples were kept at  $60^\circ\text{C}$  overnight. The pellets were then incubated with 750  $\mu\text{L}$  of demineralized water at  $100^\circ\text{C}$  for 15 min to gelatinize the starch. Starch hydrolysis was performed by adding 250  $\mu\text{L}$  (equivalent to 1200  $\text{U mL}^{-1}$  demineralized water) of a solution of heat-stable  $\alpha$ -amylase from *Bacillus licheniformis* (Sigma Aldrich GmbH, Munich, Germany). The enzyme solution was cleaned by filtration with a Vivaspin 15

regenerated cellulose membrane with a 5000 Da molecular weight cut-off (Sartorius, Göttingen Germany) to remove stabilizers. After cooling, the solutions were centrifuged (12 000 g for 5 min) and 450  $\mu\text{L}$  of supernatant was filtered with cleaned centrifugal ultrafilters (Vivaspin 500, regenerated cellulose membrane, 10 000 Da molecular weight cut-off; Sartorius). The filtered samples were used for stable carbon isotope analysis. Blanks without addition of plant material were treated in the same way as the samples. The samples were corrected for carbon content and  $\delta^{13}\text{C}$  of the blanks.

### Determination of phloem sap sugar concentrations

For the determination of soluble carbohydrates, 5–10  $\mu\text{L}$  of phloem sap was diluted to 500  $\mu\text{L}$  with demineralized water according to Keitel *et al.* (2003). One hundred microlitre aliquots were injected into a high-performance liquid chromatography system (Dionex DX 500; Dionex, Idstein, Germany). Separation of sugars was achieved on a CarboPac 1 separation column (250  $\times$  4.1 mm, Dionex) with 36 mM NaOH as an eluent at a flow rate of 1  $\text{mL min}^{-1}$ . Carbohydrates were measured by means of a pulsed amperometric detector equipped with a Au working electrode (Dionex DX 500, Dionex). Individual carbohydrates that eluted 8 to 16 min after injection were identified and quantified by internal and external standards. Sucrose was the dominant sugar in the phloem and made up >98% of the total phloem sap sugars. Sucrose carbon was related to total C in the phloem determined with an elemental analyser coupled to an isotope ratio mass spectrometer (IRMS) (see further) in order to check if the relative contribution of sucrose C changed over the diel course.

### Gas exchange measurements

For all leaves at all time points, net  $\text{CO}_2$  exchange ( $A$ ) and  $c_i/c_a$  (ratio of mole fractions of  $\text{CO}_2$  inside and outside the leaf) were determined before harvest using a portable leaf gas exchange measurement system (LCA 4; ADC BioScientific Ltd., Hoddesdon, UK). Air temperature and relative air humidity varied between approximately 28.5 and  $31.5^\circ\text{C}$  and 55 and 95%, respectively, during the diel course (Gessler *et al.* 2007a). During the light period, photosynthetically active radiation at the upper plant canopy level was between 320 and 600  $\mu\text{mol m}^{-2} \text{s}^{-1}$ .

### Isotope measurements and isotopic calculations

Carbon isotope signatures and carbon contents of oven-dried bulk plant material and the different extracts were determined using a Delta Plus IRMS (ThermoFinnigan, Bremen, Germany) coupled to an elemental analyser (NA 2500; CE Instruments, Milan, Italy) as described in detail by Keitel *et al.* (2006) and Brandes *et al.* (2006). The samples which were combusted in tin capsules (IVA

Analysentechnik, Meerbusch, Germany) contained, on average, between 200 and 400  $\mu\text{g}$  organic C. Precision of the measurements of the standard IAEA-CO-8 (International Atom Energy Agency, Vienna, Austria) was 0.11‰ (1 SD,  $n = 10$ ). Carbon isotope signatures ( $\delta^{13}\text{C}$  in ‰) are presented as the ratios of  $^{13}\text{C}/^{12}\text{C}$  of a sample relative to the Vienna Pee Dee belemnite standard.

Photosynthetic  $\text{CO}_2$  discrimination ( $\Delta_i$ ) was calculated from  $c_i/c_a$  according to the following equation (Farquhar *et al.* 1982), which describes a two-stage model (diffusion through the stomata followed by carboxylation):

$$\Delta_i = a + (b - a) \cdot \frac{c_i}{c_a} \quad (1)$$

where  $a$  is the fractionation (4.4‰) related to diffusion in air, and  $b$  is the net fractionation during  $\text{CO}_2$  fixation by Rubisco. The ordinary  $b$  value used to calculate  $\Delta_i$  is 27‰, which has been obtained through best fits of experimental  $\Delta_i$  response curves. Therefore, this value integrates the drawdown of the  $\text{CO}_2$  mole fraction from intercellular spaces to carboxylation sites. We thus used  $b = 27‰$  with Eqn 1. In an additional approach, we applied the complete model for photosynthetic carbon isotope discrimination of Farquhar *et al.* (1982) according to the following equation:

$$\Delta = a_b \frac{c_a - c_s}{c_a} + a \frac{c_s - c_i}{c_a} + (e_s + a_1) \frac{c_i - c_c}{c_a} + b \frac{c_c}{c_a} - \frac{eR_d}{k} + f\Gamma^* \quad (2)$$

where  $c_s$  and  $c_c$  are the mole fractions of  $\text{CO}_2$  on the leaf surface and in the chloroplast, respectively;  $a_b$ ,  $e_s$  and  $a_1$  are the fractionation factors associated with diffusion through the boundary layer (2.9‰), with dissolution of  $\text{CO}_2$  (0.7‰) and with diffusion of  $\text{CO}_2$  in water (1.1‰), respectively. In Eqn 2, we used a fractionation factor  $b$  of 29.5‰ [pure ribulose-1,5-bisphosphate (RuBP) carboxylation fractionation]. The symbols  $e$  and  $f$  represent the fractionations associated with day respiration  $R_d$  and with photorespiration;  $k$  is the carboxylation efficiency, and  $\Gamma^*$  is the  $\text{CO}_2$  compensation point in the absence of day respiration.

We estimated mesophyll conductance ( $g_i$ ) from its relationship with assimilation rate as shown by von Caemmerer & Evans (1991) for various  $\text{C}_3$  species, and calculated  $c_c$  from the relation  $c_c = c_i - A/g_i$ . In order to account for the uncertainty of such an estimate, we calculated  $c_c$  not only for the  $g_i$  computed as described but also for  $g_i$  values 30% greater and less. Tcherkez (2006) gave a range for  $f$  from 7.0 to 13.7%. Fractionation associated with glycine carboxylase amounts to 20‰, and is thought to roughly equal  $2f$ , so a value of 10‰ for  $f$  seems reasonable, given that  $\Gamma^*/c_a$  is approximately 0.1. The day respiratory fractionation,  $e$ , is thought to be less significant because the factor  $R_d/(kc_a)$  is so small (typically 0.02). Dark (as opposed to day) respiratory fractionation was shown to vary for several species under non-stressed condition between  $-8.1$  and  $-0.1‰$

(calculated from data in Duranceau *et al.* 1999; Ghashghaie *et al.* 2001). We used the value for dark respiratory fractionation in *R. communis* in Eqn 2, which was  $-2‰$  (Gessler *et al.*, unpublished data) and was thus well within the range of the previously observed values.

We acknowledge that  $e$  might strongly change with environmental conditions and during the day–night cycle, and the assumption of a fixed value during the day might introduce some small error in the calculations of  $\Delta$ . However, even if a variation of  $e$  between  $+10$  and  $-10‰$  is assumed (cf. Ghashghaie *et al.* 2003), the day respiration term will only vary between approximately  $+0.2$  and  $-0.2‰$ .

To calculate  $\delta^{13}\text{C}$  values of newly produced organic matter ( $\delta^{13}\text{C}_p$ ) from photosynthetic discrimination ( $\Delta_i$  or  $\Delta$ ), we applied the following equation:

$$\delta^{13}\text{C}_p = \frac{\delta^{13}\text{C}_{\text{CO}_2} - \Delta_i}{1 + \Delta_i} \quad (3)$$

$\delta^{13}\text{C}$  of  $\text{CO}_2$  ( $\delta^{13}\text{C}_{\text{CO}_2}$ ) from the greenhouse air was determined to be  $-8.0 \pm 0.3‰$  as the mean value during the diel course.

In order to calculate mean canopy  $\delta^{13}\text{C}$  values for a given time point, the carbon isotope compositions of different carbon fractions of single leaves were weighted for total leaf carbon content ( $\text{mol leaf}^{-1}$ ). To calculate mean diurnal (daytime) or diel (day and night)  $\delta^{13}\text{C}$  values, carbon isotope composition was weighted according to Cernusak, Farquhar & Pate (2005) by photosynthesis or carbon content:

$$\text{weighted } \delta^{13}\text{C} = \frac{\int A \cdot \delta^{13}\text{C} \cdot dt}{\int A \cdot dt} \text{ or } \frac{\int C\% \cdot \delta^{13}\text{C} \cdot dt}{\int C\% \cdot dt} \quad (4)$$

where  $\int A \cdot \delta^{13}\text{C}$  is the light period and  $\int C\% \cdot \delta^{13}\text{C} \cdot dt$  the light period or diel integral of the product of  $A$  and  $\delta^{13}\text{C}$ , and  $C\%$  and  $\delta^{13}\text{C}$ , respectively, and  $\int A \cdot dt$  and  $\int C\% \cdot dt$  are the light period or diel integrals of photosynthesis and carbon content.

## Isotope model

The modelling approach of Tcherkez *et al.* (2004), based on the fractionating enzymatic reactions of the primary carbon metabolism, is used here. A general scheme describing the main steps considered is given in Fig. 2. The carbon isotope composition of sucrose produced in the light or during the night is calculated with the steady-state equations (*forward modelling*) given in the Appendix of Tcherkez *et al.* (2004). Further details on the equations may be found in this reference. Briefly, the isotope ratios  $^{13}\text{C}/^{12}\text{C}$  in all the C atom positions of carbohydrate molecules are expressed in the steady-state with mass balance equations. With a substitution procedure, we obtain linear functions of the isotope ratio in C-1 of chloroplastic 3-phosphoglyceraldehyde (further denoted as  $R_G$ ).  $R_G$  is as follows:

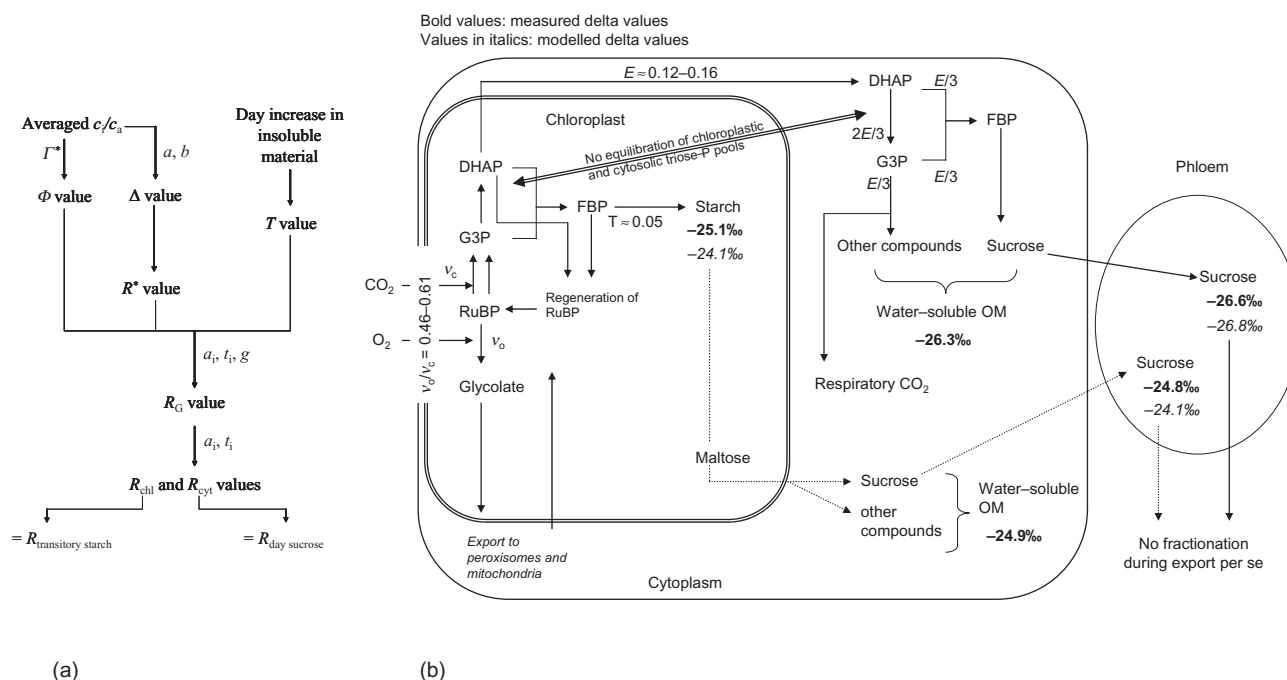


**Figure 2.** Main steps and assumptions considered in the isotopic model of Tcherkez *et al.* (2004) used in the present paper. (a) shows a brief scheme of the steps of calculations leading to the modelled isotopic ratio  $R$  of transitory starch and day sucrose. The model takes into account the fractionations of the chemical reactions that are involved in modifying C-C bonds: ribulose 1,5-bisphosphate carboxylase/oxygenase (Rubisco), (trans)aldolase, transketolase and glycine decarboxylase. (b) shows the main carbon fluxes considered in the model and gives a comparison between measured (bold) and modelled (italics) isotopic values. The starch synthesis flux (in moles of hexoses per mole of  $CO_2$  fixed) is  $T$ . Its average value is approximately 0.05 and has been determined from the rate of increase in leaf water-insoluble organic matter (IOM) during the day. Export from the chloroplast represents a flux  $E$ , from which  $E/3$  is directed to glycolysis and  $E/3$  to hexose synthesis.  $E$  ranges between approximately 0.12 and 0.16 (in moles of dihydroxyacetone phosphate per mole of  $CO_2$  fixed) and is calculated from  $v_o/v_c$  ( $= \Phi$ ) and  $T$  as follows (see Tcherkez *et al.* 2004 for details):  $E = 1/3 - \Phi/6 - 2T$ . In the cytoplasm,  $2E/3$  is consumed for sucrose synthesis and  $E/3$  for the production of other carbon compounds and for respiration. The fluxes denoted with solid arrows are day fluxes; those denoted with dotted arrows are night fluxes. Typical observed and calculated  $\delta^{13}C$  values for ratio of mole fractions of  $CO_2$  inside and outside the leaf ( $c_i/c_a$ ) = 0.7 are given in bold and italic, respectively. RuBP, ribulose-1,5-bisphosphate; G3P, 3-phosphoglycerate; DHAP, dihydroxyacetone phosphate; FBP, fructose bisphosphate;  $v_o/v_c$ , oxygenation-to-carboxylation ratio;  $\Gamma^*$ ,  $CO_2$  compensation point in the absence of dark respiration;  $\Delta$ , photosynthetic carbon isotope discrimination;  $R^*$ , isotope ratio of the carbon input;  $a_i$ , isotope effects associated with the aldolase reaction;  $t_i$ , isotope effects of the transketolase reaction;  $g$ , carbon isotope fractionation associated with photorespiratory glycine decarboxylation;  $R_G$ , isotope ratio in C-1 of chloroplastic 3-phosphoglycerate;  $R_{chl}$  and  $R_{cyt}$ , isotope ratios of chloroplastic and cytoplasmic hexoses, respectively; OM, organic matter.

$$R_G = \frac{R^*}{1 + \Phi \left( \frac{1}{2} - \frac{1}{3} \frac{1+g}{2+g} (\varepsilon + 2a_2 \tilde{a}_2 \varepsilon') \right) + T(a_4 - 1)} \quad (5)$$

$$\text{where } \tilde{a}_i = \frac{1 + \Phi/2 - T}{\frac{2a_i + 1}{3} + \Phi \frac{2a_i - 1/2}{3} + T(a_i - 2)},$$

$$\varepsilon' = \frac{(\tilde{t}_1 + 3\Phi/2)a_3 \tilde{a}_3}{3(1 + \Phi/2 - (1 + \tilde{t}_2)a_2 \tilde{a}_2/3)}$$

$$\tilde{t}_i = \frac{1 + 3T}{t_i + 3T} t_i \text{ for } i = 1, 2 \text{ or } 3, \text{ and } \varepsilon = a_3 \tilde{a}_3,$$

where  $\Phi$  is the oxygenation-to-carboxylation ratio  $v_o/v_c$ ,  $g$  the isotope fractionation associated with  $CO_2$  production from glycine (glycine decarboxylation), and  $T$  the relative flux of starch synthesis. The isotope ratio of the carbon input

( $R^*$ ) is calculated with the  $c_i/c_a$  values obtained at different times (1000, 1200, 1600, 1900 h) weighted with assimilation of the leaves placed above the phloem sap collecting point. The use of the simplified model for photosynthetic carbon isotope discrimination seems justified as the application of the more complex approach (Eqn 2) did not result in different values for the isotopic composition of primary assimilates (see RESULTS section). The photorespiration relative rate  $\Phi$  is calculated with the  $c_i$  value, assuming a Rubisco specificity factor of 90 and a  $CO_2$  compensation point in the absence of dark respiration ( $\Gamma^*$ ) of  $40 \mu\text{mol mol}^{-1}$  ( $c_i$ ). This rate is within the range 0.46–0.61. The starch synthesis rate ( $T$ ) is obtained, for each measurement time, using the rate of increase in leaf IOM during the day (source data not shown). The value obtained (in moles of hexoses directed to starch per moles of net fixed  $CO_2$ ) is near 0.05. The *inverse* isotope effects associated with the

aldolase ( $a_2, a_3, a_4$ ) and the transketolase ( $t_1, t_2$ ) reactions are those found by Tcherkez *et al.* (2004) using the isotope ratios found in glucose in typical conditions (by *reverse modelling*):  $a_2 = 1.0012$ ,  $a_3 = 1.0058$ ,  $a_4 = 1.0161$ ,  $t_1 = 0.9924$ ,  $t_2 = 1.0008$ . The isotope effect associated with glycine decarboxylation was set to 1.020 as indicated by the latter authors and Tcherkez (2006). In such a framework, the average (whole molecule) isotope ratios are

$$R_{\text{chl}} = \frac{1}{6} \left( \varepsilon' \left( 1 + \frac{a_2 \tilde{a}_2 \tilde{t}_2}{t_2} \right) + \varepsilon \left( 2 + \frac{\tilde{t}_1}{t_1} \right) + a_4 \right) R_G \quad (6)$$

in chloroplastic hexoses and transitory starch, and

$$R_{\text{cyt}} = \frac{1}{6} \left( 2\varepsilon + \frac{3(a_2 + 1)}{a_2 + 2} \varepsilon' \tilde{a}_2 + \frac{3\tilde{a}_3}{2 + a_3} \left( a_3 + \frac{2a_4}{1 + a_4} \right) \right) R_G \quad (7)$$

in cytoplasmic hexoses (and thus in day sucrose).

### Statistical approaches

All statistical analyses were performed using NCSS 2004 (Number Cruncher Statistical Software, Kaysville, UT, USA). Differences in  $\delta^{13}\text{C}$  between time points and/or different positions were determined using analysis of variance (ANOVA) (general linear model ANOVA). For variance analysis, the position was nested within a time point. Assimilation-weighted daily averages of  $\delta^{13}\text{C}$  in primary assimilates were compared with other carbon pools by applying the two-sided Student's *t*-test.

## RESULTS

### Diel courses of net photosynthesis and $c_i/c_a$

Net  $\text{CO}_2$  exchange rate was not different among leaves L3–L7 (L7: youngest leaf at the top) during the whole diel course but was significantly lower during the day in the oldest leaves L1 and L2 at the bottom of the canopy (Fig. 3). In the light, net assimilation of the upper five leaves (L3–L7) was between 6.2 and 10.6  $\mu\text{mol CO}_2 \text{ m}^{-2} \text{ s}^{-1}$  with maxima during midday and during the late afternoon. Respiratory  $\text{CO}_2$  emission in the dark ranged between 1.4 and 2.8  $\mu\text{mol CO}_2 \text{ m}^{-2} \text{ s}^{-1}$ .  $c_i/c_a$  did not differ significantly among leaves L3–L7. Leaf area-weighted mean values of  $c_i/c_a$  increased from 0.58 to 0.78 between 1030 and 1630 h and decreased again until 1900 h.

### $\delta^{13}\text{C}$ in different organic carbon pools of the leaves

In the WSOM (exportable) fraction, there were only slight differences in  $\delta^{13}\text{C}$  among leaves between 1030 and 1630 h (Fig. 4a). In the evening and during the dark period, however, a stronger gradient was observed within the canopy. The difference in  $\delta^{13}\text{C}$  between the leaves of the upper canopy and L1/L2 was up to 2.2‰. During the diel course, weighted mean canopy  $\delta^{13}\text{C}$  decreased from -26.1‰

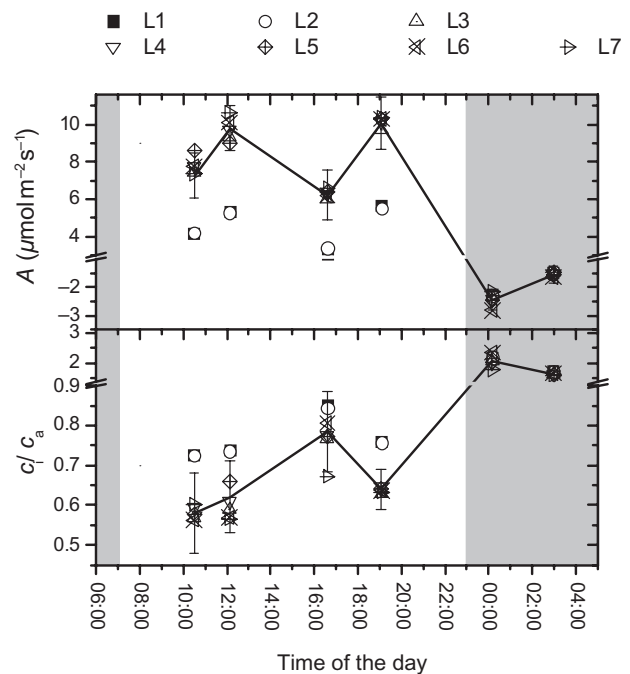


**Figure 3.** Net photosynthesis  $A$  and ratio of mole fractions of  $\text{CO}_2$  inside and outside the leaf ( $c_i/c_a$ ) of all seven leaves (L1–L7) of the examined *Ricinus communis* plants during the diel course. Data shown are mean values ( $n = 3 - 4$ ). The line refers to the leaf area-weighted mean values ( $\pm$ SD as error bars). The grey fields denote the dark period. L1 and L2 are the oldest leaves at the base of the canopy; L7 is the youngest leaf at the top (cf. Fig. 1 in Materials and Methods).

at 1030 h to ca. -26.6‰ at 1200 h. Between 1630 and 1900 h,  $\delta^{13}\text{C}$  increased by 1‰, and nocturnal values were between -24.8 and -25.0‰.

A significant increase in  $\delta^{13}\text{C}$  from the lower to the upper part of the canopy was observed in IOM (non-exportable) of leaves during the whole diel course (Fig. 4b). Maximum differences between L1 and L7 observed at 1630 h were 4.2‰. The diel pattern was inverted compared with WSOM with maxima between 1200 and 1630 h and minima during the night.

The  $\delta^{13}\text{C}$  values in the starch extracts were not significantly different among leaves L3, L4, L5 and L7 (ranging from -24.9 to -25.3‰, Table 1) and this is consistent with their similar  $c_i/c_a$  values (Fig. 3). The  $\delta^{13}\text{C}$  values of starch were similar in the light (mean value of leaves L3, L4, L5 and L7 at 1600 h:  $-25.0 \pm 0.6$ ‰) and in darkness (at 0300 h:  $-25.2 \pm 0.7$ ‰), and were comparable with mean canopy leaf WSOM in the night (Figs 2 & 4).

### $\delta^{13}\text{C}$ in organic carbon pools along the stem axis and in the roots

Within the canopy,  $\delta^{13}\text{C}$  of total organic matter (Fig. 5a) in stem sections decreased from the top (f) to the lower part (c). This gradient was most pronounced during the light period. In contrast,  $\delta^{13}\text{C}$  did not differ significantly among

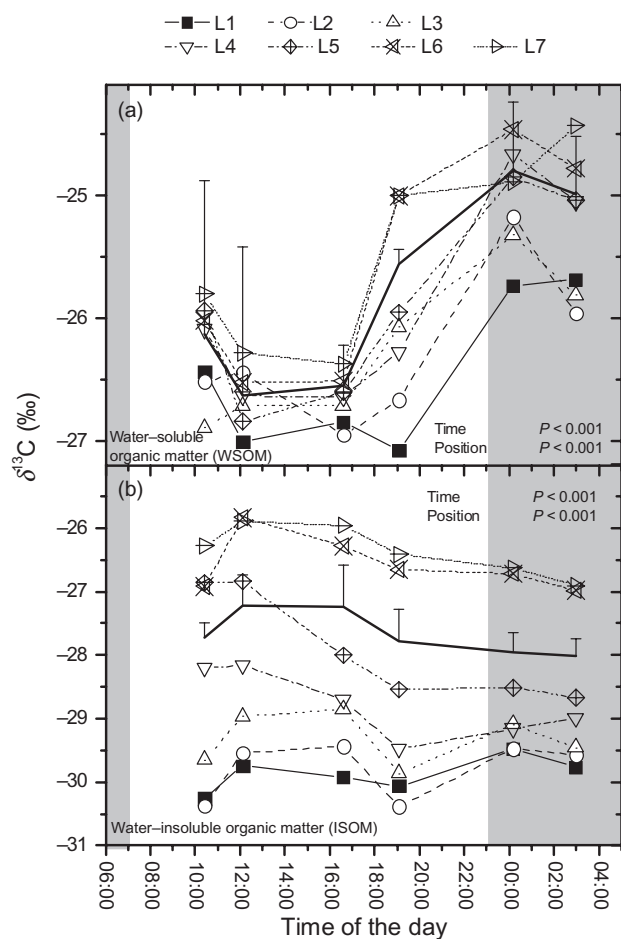


**Figure 4.**  $\delta^{13}\text{C}$  in (a) water-soluble organic matter (WSOM) and (b) non-exportable water-insoluble organic matter (IOM), in all seven leaves (L1–L7) of *Ricinus communis* during the diel course. Data shown are mean values ( $n = 3 - 4$ ). In addition, the canopy weighted mean values (bold line + SD as error bars) are displayed. To calculate canopy weighted mean values, the  $\delta^{13}\text{C}$  of single leaves was weighted for total leaf carbon content (mol leaf $^{-1}$ ). The effects of position and time as calculated with the general linear model ANOVA procedure are given. The grey fields denote the dark period.

stem sections below the leaves (a–c). Total organic carbon of fine roots was, however, enriched in  $^{13}\text{C}$  by up to 1.6‰ as compared with the lowermost stem section. There was a distinct diel pattern in  $\delta^{13}\text{C}$  values of stem sections and roots with a minimum at 1900 h and a maximum during the night and a mean peak-to-peak variation of 0.6‰.

The diel amplitude was higher for  $\delta^{13}\text{C}$  in phloem sap organic matter (Fig. 5b). Minimum  $\delta^{13}\text{C}$  values between  $-28.3$  and  $-29.9$ ‰ were observed at midday, whereas lowest  $^{13}\text{C}$  depletion occurred during the night resulting in  $\delta^{13}\text{C}$  values of  $-23.7$  to  $-24.9$ ‰. In contrast to total organic matter in stem sections, there was no difference in  $\delta^{13}\text{C}$  of phloem sap organic matter among different sampling positions. There were slight variations in sucrose carbon and total carbon concentrations during the diel course, but the

relative contribution of sucrose carbon was always around 90% (Table 2).

### Comparison of $\delta^{13}\text{C}$ of leaf and leaf-exported carbon pools

There was a highly significant negative regression relation between mean canopy-weighted  $\delta^{13}\text{C}$  of leaf IOM and (1) leaf WSOM [ $\delta^{13}\text{C}$  leaf WSOM (‰) =  $-1.97 \times \delta^{13}\text{C}$  leaf IOM (‰) - 80.3 (‰),  $R^2 = 0.94$ ,  $P = 0.0012$ ] and (2) phloem sap organic matter [ $\delta^{13}\text{C}$  phloem (‰) =  $-4.39 \times \delta^{13}\text{C}$  leaf IOM (‰) - 147.6 (‰),  $R^2 = 0.84$ ,  $P = 0.01$ , for phloem sap collected at position d directly below the canopy] during the whole diel course. This finding shows the close coupling between the water-insoluble and the two soluble pools, that is, any  $^{13}\text{C}$  enrichment in insoluble C is compensated by a  $^{13}\text{C}$  depletion in soluble C, and vice versa. In addition, the  $\delta^{13}\text{C}$  of mean canopy-weighted leaf WSOM was significantly correlated with phloem sap organic matter (at position d) [ $\delta^{13}\text{C}$  phloem (‰) =  $1.97 \times \delta^{13}\text{C}$  leaf WSOM (‰) + 24.6 (‰),  $R^2 = 0.84$ ,  $P = 0.01$ ]. The nocturnal  $\delta^{13}\text{C}$  values in leaf WSOM and phloem sap organic matter were comparable to  $\delta^{13}\text{C}$  in starch (cf. Fig. 2) indicating this carbon pool to be the source for sugars exported from the leaves to the phloem in the dark.

Photosynthesis-weighted mean daily  $\delta^{13}\text{C}$  value for primary assimilates (calculated from  $c_i/c_a$  according to Eqns 1, 3 & 4) was  $-26.3$ ‰ (Fig. 6). When taking into account fractionation associated with photorespiration and day respiration as well as estimated mesophyll conductance and  $c_c$  for calculating photosynthetic discrimination, the  $\delta^{13}\text{C}$  for primary assimilates amounted to  $-25.9$ ‰ and thus did not strongly differ from the  $c_i/c_a$  derived value. The grey bar in Fig. 6 shows the range for  $g_i$  values being 30% higher and lower than the one calculated according to von Caemmerer & Evans (1991). The value calculated from  $c_i/c_a$  did not differ significantly from the  $\delta^{13}\text{C}$  of the leaf WSOM and the phloem sap carbon pool averaged over the light

**Table 1.** Carbon isotope composition of starch extracted from different leaves at two time points

|      | 1600 h (day)        | 0300 h (night)      |
|------|---------------------|---------------------|
| L7   | $-24.9 \pm 0.3$ a A | $-25.1 \pm 0.5$ a A |
| L5   | $-24.9 \pm 0.3$ a A | $-25.2 \pm 0.4$ a A |
| L4   | $-25.0 \pm 1.0$ a A | $-25.2 \pm 0.9$ a A |
| L3   | $-25.1 \pm 0.9$ a A | $-25.3 \pm 0.8$ a A |
| Mean | $-25.0 \pm 0.6$ A   | $-25.2 \pm 0.7$ A   |

The position of leaves L3, L4, L5 and L7 is given in Fig. 1. Data shown are mean values ( $\pm$ SD) in parts ‰ ( $n = 4$ ). The mean value per time point is weighted for leaf area. Different leaves at a given time point that share the common lower case letter 'a' are not significantly different [one-way analysis of variance (ANOVA) with Tukey–Kramer post hoc test,  $P < 0.05$ ] in  $\delta^{13}\text{C}$ . Leaves from the same position (and mean values) that share the common upper case letter 'A' are not different between the two different time points (Student's  $t$ -test,  $P < 0.05$ ).

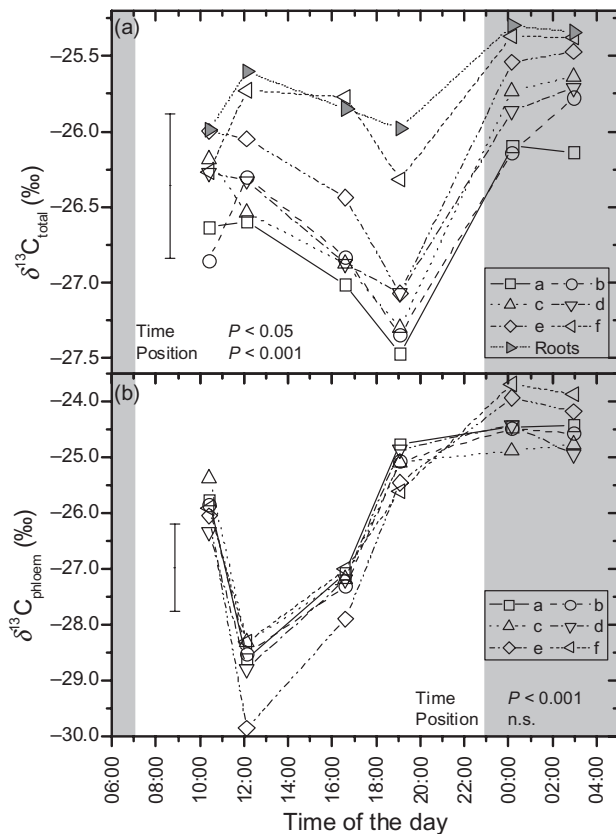


**Figure 5.**  $\delta^{13}\text{C}$  in total organic matter in stem sections and fine roots (a) and in phloem sap organic matter (b) along the axis (a–f) of *Ricinus communis* during the diel course. Position a denotes the sampling position at the stem base; f is the uppermost stem position harvested (cf. Fig. 1; Materials and Methods). Data shown are mean values ( $n = 3\text{--}4$ ). The average standard errors of the mean values for all tissues sections and time points are given as error bars. In addition, effects of position along the axis and time on  $\delta^{13}\text{C}$  as calculated with the general linear model ANOVA procedure are given. n.s., not significant.

period, but was significantly  $^{13}\text{C}$  enriched compared with daytime total organic matter and IOM. During the night, both phloem sap and leaf WSOM were significantly  $^{13}\text{C}$  enriched compared with daytime primary assimilates calculated from  $c_i/c_a$ . Integrated over the whole diel course, the non-exportable carbon was significantly depleted in  $^{13}\text{C}$  compared with the newly assimilated organic carbon,

whereas the leaf exportable and the phloem sap fraction were slightly albeit not significantly enriched.

### Comparison of the $\delta^{13}\text{C}$ values with the predicted day/night oscillations

The  $\delta^{13}\text{C}$  values of the organic matter transported in the phloem may be predicted, assuming that (1) during the light period, phloem sap organic matter essentially contains sucrose produced in the light through triose phosphates aldolization and sucrose synthesis, and (2) during the night, phloem sap organic matter comes from the degradation of transitory starch into sucrose (cf. Fig. 2). Using  $c_i/c_a$  values to obtain the isotopic composition of photosynthetic  $\text{CO}_2$  input, the  $\delta^{13}\text{C}$  values of both day and night sucrose were calculated (see Materials and Methods). The results are shown as a function of time in Fig. 7a. The predicted values are very similar for all the a, d, e and f levels, and Fig. 7a shows the calculated time course associated with stem position f only. The model predicts a large oscillation of the phloem  $\delta^{13}\text{C}$  value, and this is more or less consistent with the observed values.

Figure 7, inset in panel b gathers all the data points associated with the four different levels, a, d, e and f, into day and night values, and predicted values are plotted against the observed ones. It can be seen that the relationship is within the 1:1 neighbourhood. A linear regression analysis yielded an  $R^2$  of 0.25 ( $P = 0.017$ ). The remaining variability virtually disappears when average day and night values are used (Fig. 7b,  $R^2 = 0.95$ ,  $P < 0.001$ ). This indicates that the model satisfactorily accounts for the diel  $^{13}\text{C}$  oscillations, but this may be better demonstrated with average values, simply because phloem sap organic matter integrates the carbon input from leaves rather slowly (see DISCUSSION section).

### Comparison between $\delta^{13}\text{C}$ of carbon pools along the axis

Mean diel  $\delta^{13}\text{C}$  did not differ in the phloem sap organic matter among sampling positions but decreased in total organic carbon of stem sections in the basipetal direction along the stem (Table 3). These patterns resulted in total carbon of stem sections being significantly  $^{13}\text{C}$  depleted as compared with phloem sap organic matter at the stem base (axis position a). The mean diel  $\delta^{13}\text{C}$  in total carbon in fine

| Time of the day | Sucrose C concentration (M) | Total C concentration (M) | Sucrose C: total C |
|-----------------|-----------------------------|---------------------------|--------------------|
| 1030 h          | $3.46 \pm 0.28$             | $3.79 \pm 0.45$           | $0.91 \pm 0.12$    |
| 1200 h          | $3.66 \pm 0.22$             | $4.02 \pm 0.33$           | $0.91 \pm 0.08$    |
| 1630 h          | $3.58 \pm 0.25$             | $3.95 \pm 0.43$           | $0.91 \pm 0.12$    |
| 1900 h          | $3.59 \pm 0.18$             | $4.03 \pm 0.39$           | $0.89 \pm 0.10$    |
| 2400 h          | $3.46 \pm 0.23$             | $3.77 \pm 0.25$           | $0.92 \pm 0.08$    |
| 0300 h          | $3.30 \pm 0.20$             | $3.74 \pm 0.32$           | $0.88 \pm 0.09$    |

**Table 2.** Sucrose carbon and total carbon concentration and relative contribution of sucrose carbon to total carbon in the phloem sap of *Ricinus communis* during the diel course

Data shown are mean values  $\pm$  SE from phloem sampling position C (see Fig. 1).  $n = 3\text{--}4$ .



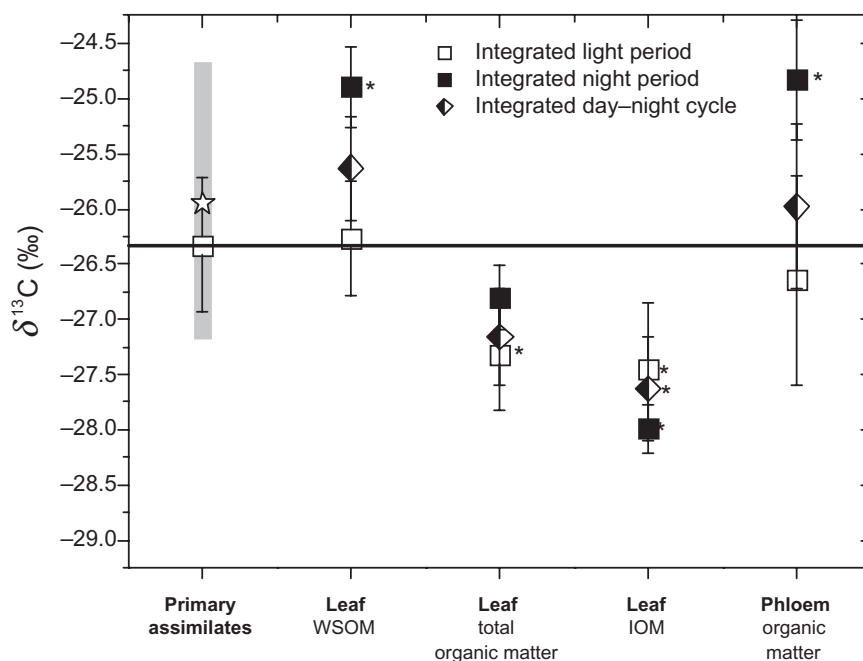


**Figure 6.** Mean daytime  $\delta^{13}\text{C}$  of primary assimilates compared with mean  $\delta^{13}\text{C}$  of foliar water-soluble organic matter (WSOM), total and water-insoluble organic matter (IOM) as well as to phloem sap organic matter during the light and dark period and during the full day–night cycle. The  $\delta^{13}\text{C}$  of primary assimilates was calculated according to Eqns 1 and 3 and was weighted for the assimilation rate (Eqn 4). The star shows the calculated mean daytime  $\delta^{13}\text{C}$  value of primary assimilates taking into account the chloroplastic  $\text{CO}_2$  concentration ( $c_c$ ) as well as fractionation because of photorespiration and day respiration (Eqn 2).  $c_c$  was estimated with a  $g_i$  value as calculated according to von Caemmerer & Evans (1991). The grey bar covers the range of calculated daytime mean  $\delta^{13}\text{C}$  when  $g_i$  values 30% higher and lower than the value calculated according to von Caemmerer & Evans (1991) were assumed. The  $\delta^{13}\text{C}$  of the different other fractions in leaves were weighted for carbon content (cf. Eqn 4). The  $\delta^{13}\text{C}$  of the phloem sap organic matter sampled below the canopy (position c cf. Fig. 1, Materials and Methods) was weighted for time and phloem sap carbon content. Data shown are mean values  $\pm$ SD from three to four plants. \* indicates significant differences from primary assimilates calculated according to Eqn 1 (Student's  $t$ -test,  $P < 0.05$ ).

roots was more positive compared with total carbon at the stem base and was slightly – albeit not significantly –  $^{13}\text{C}$  enriched as compared with phloem sap organic matter.

## DISCUSSION

In the present study, we aimed at characterizing post-carboxylation carbon isotope fractionation in leaves during the diel course and its effect on  $\delta^{13}\text{C}$  of carbon pools within and exported from leaves. For this purpose, we measured the carbon isotope composition of exportable and non-exportable leaf and phloem sap organic matter and compared the values with the ones calculated with a model, taking into account the carbon isotope fractionations in the reactions of the primary carbon metabolism (Tcherkez *et al.* 2004, Materials and Methods and Fig. 2). In order to assess potential fractionation in heterotrophic tissues, we characterized the  $\delta^{13}\text{C}$  of phloem sap organic matter along the axis and compared it with total organic matter in stem segments and fine roots of *R. communis*.

### The circadian rhythm of $\delta^{13}\text{C}$ values in phloem organics

Clearly, the present study shows that there is a circadian rhythm of the  $^{13}\text{C}$  abundance in leaf WSOM and in phloem

sap, that is, in organic molecules exported by leaves (Figs 4b & 5b). This phenomenon was predicted by Tcherkez *et al.* (2004) on a metabolic basis. Briefly, during the light period, the production of sucrose in the cytoplasm involves  $^{13}\text{C}$ -depleted triose phosphates exported from the chloroplast. The  $^{13}\text{C}$  depletion is a consequence of transitory starch synthesis, which favours  $^{13}\text{C}$  during intra-chloroplastic fructose production by aldolase (Gleixner & Schmidt 1997). During the night, sucrose synthesis involves starch degradation and, so, uses  $^{13}\text{C}$ -enriched carbon. As a result, an oscillation between light- and dark-exported sucrose is expected (Fig. 2).

The comparison of the observed values of phloem sap organic matter to  $\delta^{13}\text{C}$  calculated using the model of Tcherkez *et al.* (2004) is shown in Fig. 7. While the model reproduces well the range in which day and night values vary, there are some discrepancies along the time course (Fig. 7a). As a result, there is some noise around the 1:1 relationship between observed and predicted values (Fig. 7b, inset). Nevertheless, we note that this is almost eliminated when day and night average values are used. This reflects the fact that the predicted values calculated with instantaneous  $c_i/c_a$  measured values (photosynthesis weighted for several leaves) cannot fully account for the phloem sap organic matter  $^{13}\text{C}$  content. This effect might originate from (1) a lag phase

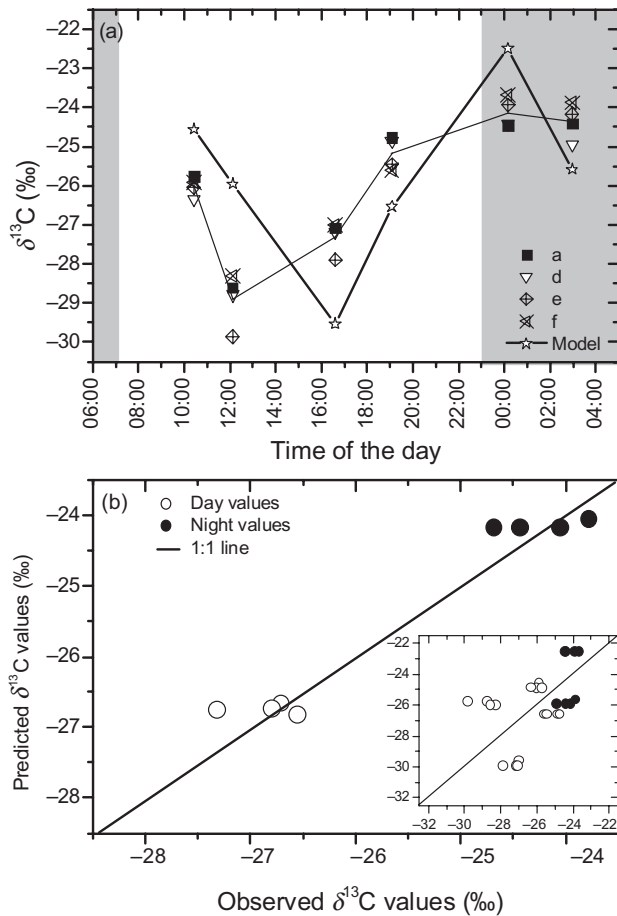


**Figure 7.** Comparison of observed  $\delta^{13}\text{C}$  values of phloem sap sugars collected in the present study with the values predicted using the model of Tcherkez *et al.* (2004) for day sucrose (day values) and transitory starch (night values). (a) Time course of both observed (stem positions a, d, e and f; the thin line denotes the mean value for the four positions) and predicted values (stars). The day values take into account the photosynthesis-weighted average of ratio of mole fractions of  $\text{CO}_2$  inside and outside the leaf of leaves above the phloem collecting point. The night values take into account the lag phase associated with the degradation of the most recent starch first, because of the lamellar structure of leaf transitory starch. For further details, see the section Materials and Methods. To facilitate the readability of the graph, the predicted values are shown for level f only. The other predicted values are very similar (within  $\pm 0.15\text{‰}$ ). The grey fields denote the dark period. (b) Relationship between observed and predicted values by plotting them against each other, using the average day (open symbols) and night (closed symbols) values obtained at the different plant levels. Inset: relationship between observed and predicted values by plotting them against each other using data from single time points instead of day and night averages. As in (b), open symbols denote day, and closed symbols denote night values. The straight lines show the 1:1 relationship.

between the instantaneous production of photosynthates and phloem accumulation in the stem because of a turnover time of leaf sugars in *Ricinus* amounting to approximately 2 h (Gessler *et al.* 2007a) plus the time needed to transfer newly assimilated photosynthates from the leaf to the

phloem cells (as observed by Barbour *et al.* 2000 and Keitel *et al.* 2003 with isotopic techniques), which the model does not account for, and (2) the probable heterogeneous export efficiency of the different leaves (Jeschke & Pate 1991). The prevalence of a given leaf in exported phloem material affects the overall  $^{13}\text{C}$  abundance, if its  $c_i/c_a$  value is not very close to the average  $c_i/c_a$  value. Another reason for our observation might be (3) the complexity of the phloem network, which may introduce carbon from leaves below the phloem collecting points (Turgeon 2006). As sucrose made up approximately 90% of the carbon transported in the phloem as also observed previously by Peuke *et al.* (2001) and the sucrose proportion did not change over the diel course, there is no reason to assume that changes in the chemical composition of the phloem sap are responsible for the variations observed in  $\delta^{13}\text{C}$ .

### The relationship with leaf carbohydrates

There is also a (modest) circadian rhythm of the  $\delta^{13}\text{C}$  value of leaf IOM (Fig. 4b). This is likely the result of starch accumulation (increase of  $\delta^{13}\text{C}$  in the morning) and remobilization (slight decrease of  $\delta^{13}\text{C}$  at night). The inverse correlation between  $\delta^{13}\text{C}$  in leaf IOM and leaf WSOM or phloem sap organic matter (see Results) indeed reflects the influence of diel starch dynamics on  $^{13}\text{C}$  enrichment or depletion in phloem-transported sugars. This is consistent with the fact that the carbon isotope composition of phloem sap organic matter equals that of starch in the night-time (cf. Fig. 2). The present diel cycle of  $\delta^{13}\text{C}$  in phloem organic matter and its correlation with starch dynamics is in strong agreement with previous observations. In sunflower, Ghashghaie *et al.* (2001) determined differences in the  $\delta^{13}\text{C}$  of foliar sucrose between light and dark periods of ca. 1‰, with  $\delta^{13}\text{C}$  values at night being close to those of starch. Brandes *et al.* (2006) report day–night differences in the  $\delta^{13}\text{C}$  of phloem exudates of  $>1\text{‰}$  with *Pinus sylvestris*. The authors showed that the increase in the  $\delta^{13}\text{C}$  of phloem-transported organic matter during the night was associated with starch breakdown. Gessler *et al.* (2007b) observed that the  $\delta^{13}\text{C}$  signatures of phloem sap organic matter in *Eucalyptus delegatensis* followed the carbon isotope composition of carbon released from starch in the dark period.

Unsurprisingly, we note that the diel oscillation in  $\delta^{13}\text{C}$  was more pronounced in phloem sap than in leaf WSOM (Figs 4 & 5); this effect is simply the consequence of different compositions of the carbon pools: phloem-transported organic matter of many plant species including *R. communis* (Pate *et al.* 1998; Peuke *et al.* 2001; Keitel *et al.* 2003) mainly consists of sucrose (Table 2), while WSOM is more heterogeneous and contains various carbohydrates, organic acids, amino acids with potentially various turnover times (Brandes *et al.* 2006).

### $^{12}\text{C}/^{13}\text{C}$ distribution within the plant

The diel rhythm of carbon accumulation in the light and remobilization in the dark period has a consequence for the

| Axis position/tissue | $\delta^{13}\text{C}$ (‰) phloem sap organic matter | $\delta^{13}\text{C}$ (‰) total organic matter | Difference between pools |
|----------------------|---|--|--------------------------|
| Stem f               | $-25.8 \pm 0.6 \alpha$                              | $-25.8 \pm 0.5 \alpha\beta$                    |                          |
| Stem c               | $-25.8 \pm 0.7 \alpha$                              | $-26.4 \pm 0.4 \beta\chi$                      |                          |
| Stem a               | $-26.0 \pm 0.5 \alpha$                              | $-26.7 \pm 0.4 \chi$                           | *                        |
| Roots                | $-26.0 \pm 0.5^a$                                   | $-25.7 \pm 0.3 \alpha$                         |                          |

**Table 3.** Mean diel  $\delta^{13}\text{C}$  of phloem sap organic matter compared with total organic matter of stems and roots

<sup>a</sup> $\delta^{13}\text{C}$  of phloem sap organic matter at stem position a.

Phloem sap and stem total organic matter are compared at three positions along the stem (cf. Fig. 1, Materials and Methods). Position f is within the canopy, c directly below the canopy and a at the stem base.  $\delta^{13}\text{C}$  of fine root total carbon is compared with the isotope composition of phloem sap organic matter at position a.  $\delta^{13}\text{C}$  has been weighted for carbon content and time (Eqn 4). Greek letters indicate homogenous groups for phloem sap organic matter and total organic matter among different sample positions (general linear model ANOVA with a Tukey–Kramer post hoc test,  $P < 0.05$ ). The asterisk in column four indicates significant differences (Student's *t*-test,  $P < 0.05$ ) between phloem sap and stem total organic matter at a given position.

$\delta^{13}\text{C}$  value of the different leaf carbon pools, and, by integration over time, for the isotopic composition of leaf material compared with the exported material. The mean diurnal, nocturnal and diel  $\delta^{13}\text{C}$  values of different carbon pools calculated according to Eqn 4 are shown in Fig. 6. Whereas during the light period  $\delta^{13}\text{C}$  of exportable (leaf WSOM) and exported organic carbon (in the phloem sap) did not differ significantly from 'primary assimilates' (i.e. net assimilated carbon, calculated with  $c_i/c_a$ ), both exportable and phloem sap fractions were slightly isotopically heavier than net assimilated carbon when night values were included. On a mass balance basis, it means that, integrated over the whole day, an amount of lighter carbon remains in the leaves (IOM in Fig. 6). Taking into account photorespiration and day respiration as well as the drawdown of the  $\text{CO}_2$  concentration between the leaf intercellular spaces and the chloroplast for calculating photosynthetic fractionation did not change this picture (Fig. 6, left-hand side) as the simplified model used a lesser value for the effective fractionation by Rubisco.

In different plant species, post-carboxylation carbon isotope fractionation was also postulated to take place in the stem (Terwilliger *et al.* 2001; Helle & Schleser 2004). We observed a tendency for total carbon along the plant axis to be increasingly  $^{13}\text{C}$  depleted as compared with the respective carbon source (phloem sap organic matter) in the basipetal direction (Table 3). As lignification is more pronounced at the stem base because of secondary thickening, a more intensive allocation of phloem-released carbon to this generally  $^{13}\text{C}$  depleted pool (Hobbie & Werner 2004) might explain the observed pattern.

Phloem sap organic matter, however, did not show changes in  $\delta^{13}\text{C}$  as it was transported in the basipetal direction, which is in contrast to the observations in various woody species of  $^{13}\text{C}$  enrichment of phloem-transported sugars from the twigs to the trunk base (Gessler *et al.* 2004; Brandes *et al.* 2007). Our results point to the fact that the continuous phloem unloading and partial retrieval of sugars along the transport path, which is postulated to be a major characteristic of assimilate transport in the sieve tubes

(Minchin & Thorpe 1987; Van Bel 2003), does not result in  $^{13}\text{C}$  enrichment in the stem of *R. communis*. It remains to be clarified if these differences among species are due to different transport distances, differences in metabolic processes in the stems/trunks and/or differences in phloem loading/unloading mechanisms.

In contrast to the lower stem sections, the  $\delta^{13}\text{C}$  of root total organic carbon was not significantly different in  $\delta^{13}\text{C}$  from the carbon source (i.e. phloem sap organic matter at the lowermost stem position, Table 3). The difference between mean diel  $\delta^{13}\text{C}$  of leaf ( $-27.2\text{‰}$ ) and root total organic matter ( $-25.7\text{‰}$ ), which is in agreement with the literature results compiled by Badeck *et al.* (2005), may, in our case, be due to fractionation processes during carbon export from the leaves with isotopically lighter carbon remaining in the autotrophic tissues (Fig. 6). When we assume that phloem carbon is transferred to the roots unidirectionally with no recycling of carbon from the roots to the shoots (with other potential fractionation steps),  $\delta^{13}\text{C}$  of the root sink tissue should be the same as  $\delta^{13}\text{C}$  of the source for organic carbon. However, there are recent indications that carbohydrates are also transported from the roots in the acropetal direction (Heizmann *et al.* 2001). We also recognize that other processes such as the production of  $^{13}\text{C}$ -depleted respired  $\text{CO}_2$  (associated with  $\text{CO}_2$  re-fixation by phosphoenolpyruvate carboxylase) in roots may contribute to this effect (Badeck *et al.* 2005; Klumpp *et al.* 2005; Bathellier *et al.* 2008).

### Consequences for isotope ecology

The present study provides experimental evidence that the modelling approach developed by Tcherkez *et al.* (2004), which takes into account isotope fractionation of enzymatic reactions of the primary carbon metabolism, satisfactorily predicts the day–night differences in  $\delta^{13}\text{C}$  of leaf-exported carbon in *R. communis*. We have tested the modelling approach with one species, but there is evidence that comparable day–night variations related to the transitory starch metabolism occur with other species (e.g. Tcherkez *et al.*

2004; Gessler *et al.* 2007b) Under the assumption that the cyclic nature is a general pattern in plants, it has important ramifications in isotopic ecophysiology.

Firstly, if such diel patterns were to occur in trees, the interpretation of tree ring isotope data would have to take post-carboxylation events into account (for a quantitative analysis, see Tcherkez, Ghashghaie & Griffiths 2007). For example, because phloem-transported sugars are the main C source for organic matter production in trunks, diel variations in  $\delta^{13}\text{C}$  may also affect the carbon isotope composition of whole wood or cellulose in tree rings. We know that there are indeed diel variations in the expression of key enzymes of lignin biosynthesis in herbaceous plants (Rogers *et al.* 2005). Even though uncertainty remains about such a circadian regulation of cellulose and lignin synthesis in trees, the cycling of ring deposition with phloem sap  $\delta^{13}\text{C}$  oscillations would affect the carbon isotope composition of tree rings and cause deviations from the values calculated from  $c_i/c_a$ .

Secondly, diel variations in  $\delta^{13}\text{C}$  of phloem-transported organic matter, which serves as potential substrate for respiration in heterotrophic plant parts, may also have implications for the partitioning of ecosystem  $\text{CO}_2$  fluxes using isoflux approaches (Bowling *et al.* 2001). These approaches often assume  $\delta^{13}\text{C}$  of ecosystem-emitted  $\text{CO}_2$  to be constant over day–night cycles. Only recently, this prerequisite has been shown not always to be valid (Werner *et al.* 2006). A mechanistic understanding of variations in  $\delta^{13}\text{C}$  of assimilates as affected by post-carboxylation fractionation processes might at least partially help to explain temporal dynamics in the  $\delta^{13}\text{C}$  of respired  $\text{CO}_2$  and thus might help to improve measurement and sampling strategies for isoflux approaches.

Studies are thus needed to further specify carbon transport/flux pathways within different plant species including trees in order to build mechanistic models that are better representations of the carbon metabolism of these organisms.

## ACKNOWLEDGMENTS

We would like to thank Kristine Haberer for critical reading of the manuscript and Cristiane Loyola Eisfeld for technical assistance. A.G. acknowledges financial support by a research fellowship from the Deutsche Forschungsgemeinschaft (DFG) under contract number GE 1090/4-1 and by a DFG research grant (GE 1090/5-1). G.D.F. acknowledges the Australian Research Council for its support.

## REFERENCES

- Badeck F.W., Tcherkez G., Nogue S., Piel C. & Ghashghaie J. (2005) Post-photo synthetic fractionation of stable carbon isotopes between plant organs – a widespread phenomenon. *Rapid Communications in Mass Spectrometry* **19**, 1381–1391.
- Barbour M.M., Schurr U., Henry B.K., Wong S.C. & Farquhar G.D. (2000) Variation in the oxygen isotope ratio of phloem sap sucrose from castor bean. Evidence in support of the Péclet effect. *Plant Physiology* **123**, 671–679.
- Barbour M.M., Hunt J.E., Dungan R.J., Turnbull M.H., Brailsford G.W., Farquhar G.D. & Whitehead D. (2005) Variation in the degree of coupling between  $\delta^{13}\text{C}$  of phloem sap and ecosystem respiration in two mature *Nothofagus* forests. *New Phytologist* **166**, 497–512.
- Bathellier C., Badeck F.W., Couzi P., Harscoët S., Mauve C. & Ghashghaie J. (2008) Divergence in  $\delta^{13}\text{C}$  of organic matter and respired  $\text{CO}_2$  during transition between autotrophy and heterotrophy in *Phaseolus vulgaris* L. *New Phytologist* **177**, 406–418.
- Bowling D.R., Tans P.P. & Monson R.K. (2001) Partitioning net ecosystem carbon exchange with isotopic fluxes of  $\text{CO}_2$ . *Global Change Biology* **7**, 127–145.
- Brandes E., Kodama N., Whittaker K., Weston C., Rennenberg H., Keitel C., Adams M.A. & Gessler A. (2006) Short-term variation in the isotopic composition of organic matter allocated from the leaves to the stem of *Pinus sylvestris*: effects of photosynthetic and postphotosynthetic carbon isotope fractionation. *Global Change Biology* **12**, 1922–1939.
- Brandes E., Wenninger J., Koeniger P., Schindler D., Rennenberg H., Leibundgut C., Mayer H. & Gessler A. (2007) Assessing environmental and physiological controls over water relations in a Scots pine (*Pinus sylvestris* L.) stand through analyses of stable isotope composition of water and organic matter. *Plant, Cell & Environment* **30**, 113–127.
- von Caemmerer S. & Evans J.R. (1991) Determination of the average partial pressure of  $\text{CO}_2$  in chloroplasts from leaves of several  $\text{C}_3$  plants. *Australian Journal of Plant Physiology* **18**, 287–305.
- Cernusak L.A., Farquhar G.D. & Pate J.S. (2005) Environmental and physiological controls over oxygen and carbon isotope composition of Tasmanian blue gum, *Eucalyptus globulus*. *Tree Physiology* **25**, 129–146.
- Duranceau M., Ghashghaie J., Badeck F., Deleens E. & Cornic G. (1999)  $\delta^{13}\text{C}$  of  $\text{CO}_2$  respired in the dark in relation to leaf carbohydrates in *Phaseolus vulgaris* L. under progressive drought. *Plant, Cell & Environment* **22**, 515–523.
- Farquhar G.D., O'Leary M.H. & Berry J.A. (1982) On the relationship between carbon isotope discrimination and the intercellular carbon-dioxide concentration in leaves. *Australian Journal of Plant Physiology* **9**, 121–137.
- Farquhar G.D., Ehleringer J.R. & Hubick K.T. (1989) Carbon isotope discrimination and photosynthesis. *Annual Review of Plant Physiology and Plant Molecular Biology* **40**, 503–537.
- Gessler A., Rennenberg H. & Keitel C. (2004) Stable isotope composition of organic compounds transported in the phloem of European beech – evaluation of different methods of phloem sap collection and assessment of gradients in carbon isotope composition during leaf-to-stem transport. *Plant Biology* **6**, 721–729.
- Gessler A., Peuke A.D., Keitel C. & Farquhar G.D. (2007a) Oxygen isotope enrichment of organic matter in *Ricinus communis* during the diel course and as affected by assimilate transport. *New Phytologist* **174**, 600–613.
- Gessler A., Keitel C., Kodama N., Weston C., Winters A.J., Keith H., Grice K., Leuning R. & Farquhar G.D. (2007b)  $\delta^{13}\text{C}$  of organic matter transported from the leaves to the roots in *Eucalyptus delegatensis* – short-term variations and relation to respired  $\text{CO}_2$ . *Functional Plant Biology* **34**, 692–706.
- Ghashghaie J., Duranceau M., Badeck F.W., Cornic G., Adeline M.T. & Deleens E. (2001)  $\delta^{13}\text{C}$  of  $\text{CO}_2$  respired in the dark in relation to  $\delta^{13}\text{C}$  of leaf metabolites: comparison between *Nicotiana sylvestris* and *Helianthus annuus* under drought. *Plant, Cell & Environment* **24**, 505–515.
- Ghashghaie J., Badeck F.W., Lanigan G., Nogués S., Tcherkez G., Deléens E., Cornic G. & Griffiths H. (2003) Carbon isotope

- discrimination during dark respiration and photorespiration in C<sub>3</sub> plants. *Phytochemistry Reviews* **2**, 145–161.
- Gleixner G. & Schmidt H.L. (1997) Carbon isotope effects on the fructose-1,6-bisphosphate aldolase reaction, origin for non-statistical C-13 distributions in carbohydrates. *Journal of Biological Chemistry* **272**, 5382–5387.
- Gleixner G., Scrimgeour C., Schmidt H.L. & Viola R. (1998) Stable isotope distribution in the major metabolites of source and sink organs of *Solanum tuberosum* L.: a powerful tool in the study of metabolic partitioning in intact plants. *Planta* **207**, 241–245.
- Göttlicher S., Knohl A., Wanek W., Buchmann N. & Richter A. (2006) Short-term changes in carbon isotope composition of soluble carbohydrates and starch: from canopy leaves to the root system. *Rapid Communications in Mass Spectrometry* **20**, 653–660.
- Heizmann U., Kreuzwieser J., Schnitzler J.P., Brüggemann N. & Rennenberg H. (2001) Assimilate transport in the xylem sap of pedunculate oak (*Quercus robur*). *Plant Biology* **3**, 132–138.
- Helle G. & Schleser G.H. (2004) Beyond CO<sub>2</sub>-fixation by Rubisco – an interpretation of <sup>13</sup>C/<sup>12</sup>C variations in tree rings from novel intra-seasonal studies on broad-leaf trees. *Plant, Cell & Environment* **27**, 367–380.
- Hobbie E.A. & Werner R.A. (2004) Intramolecular, compound-specific, and bulk carbon isotope patterns in C<sub>3</sub> and C<sub>4</sub> plants: a review and synthesis. *New Phytologist* **161**, 371–385.
- Jeschke W.D. & Pate J.S. (1991) Modeling of the partitioning, assimilation and storage of nitrate within root and shoot organs of castor bean (*Ricinus Communis* L.). *Journal of Experimental Botany* **42**, 1091–1103.
- Keitel C., Adams M.A., Holst T., Matzarakis A., Mayer H., Rennenberg H. & Gessler A. (2003) Carbon and oxygen isotope composition of organic compounds in the phloem sap provides a short-term measure for stomatal conductance of European beech (*Fagus sylvatica* L.). *Plant, Cell & Environment* **26**, 1157–1168.
- Keitel C., Matzarakis A., Rennenberg H. & Gessler A. (2006) Carbon isotopic composition and oxygen isotopic enrichment in phloem and total leaf organic matter of European beech (*Fagus sylvatica* L.) along a climate gradient. *Plant, Cell & Environment* **29**, 1492–1507.
- Klump K., Schäufele R., Lötscher M., Lattanzi F.A., Feneis W. & Schnyder H. (2005) C-isotope composition of CO<sub>2</sub> respired by shoots and roots: fractionation during dark respiration? *Plant, Cell & Environment* **28**, 241–250.
- Knohl A., Werner R.A., Brand W.A. & Buchmann N. (2005) Short-term variations in  $\delta^{13}\text{C}$  of ecosystem respiration reveals link between assimilation and respiration in a deciduous forest. *Oecologia* **142**, 70–82.
- Minchin P.E.H. & Thorpe M.R. (1987) Measurement of unloading and reloading of photo-assimilate within the stem of bean. *Journal of Experimental Botany* **38**, 211–220.
- Pataki D.E., Ehleringer J.R., Flanagan L.B., Yakir D., Bowling D.R., Still C.J., Buchmann N., Kaplan J.O. & Berry J.A. (2003) The application and interpretation of Keeling plots in terrestrial carbon cycle research. *Global Biogeochemical Cycles* **17**, 1022.
- Pate J., Shedley E., Arthur D. & Adams M. (1998) Spatial and temporal variations in phloem sap composition of plantation-grown *Eucalyptus globulus*. *Oecologia* **117**, 312–322.
- Peuke A.D., Rokitta M., Zimmermann U., Schreiber L. & Haase A. (2001) Simultaneous measurement of water flow velocity and solute transport in xylem and phloem of adult plants of *Ricinus communis* over a daily time course by nuclear magnetic resonance spectrometry. *Plant, Cell & Environment* **24**, 491–503.
- Rogers L.A., Dubos C., Cullis I.F., Surman C., Poole M., Willment J., Mansfield S.D. & Campbell M.M. (2005) Light, the circadian clock, and sugar perception in the control of lignin biosynthesis. *Journal of Experimental Botany* **56**, 1651–1663.
- Schmidt H.L. (2003) Fundamentals and systematics of the non-statistical distributions of isotopes in natural compounds. *Naturwissenschaften* **90**, 537–552.
- Schmidt H.L. & Gleixner G. (1998) Carbon isotope effects on key reactions in plant metabolism and <sup>13</sup>C-patterns in natural compounds. In *Stable Isotopes – Integration of Biological, Ecological and Geochemical Processes* (ed. H. Griffiths), pp. 13–25. Bios Scientific Publishers Ltd, Oxford, UK.
- Tcherkez G. (2006) How large is the carbon isotope fractionation of the photorespiratory enzyme glycine decarboxylase? *Functional Plant Biology* **33**, 911–920.
- Tcherkez G. & Farquhar G.D. (2005) Carbon isotope effect predictions for enzymes involved in the primary carbon metabolism of plant leaves. *Functional Plant Biology* **32**, 277–291.
- Tcherkez G., Farquhar G., Badeck F. & Ghashghaie J. (2004) Theoretical considerations about carbon isotope distribution in glucose of C<sub>3</sub> plants. *Functional Plant Biology* **31**, 857–877.
- Tcherkez G., Ghashghaie J. & Griffiths H. (2007) Methods for improving the visualization and deconvolution of isotopic signals. *Plant, Cell & Environment* **30**, 887–891.
- Terwilliger V.J., Kitajima K., Le Roux-Swarthout D.J., Mulkey S. & Wright S.J. (2001) Influences of heterotrophic and autotrophic resource use on carbon and hydrogen isotopic compositions of tropical tree leaves. *Isotopes in Environmental and Health Studies* **37**, 133–160.
- Turgeon R. (2006) Phloem loading: how leaves gain their independence. *Bioscience* **56**, 15–24.
- Van Bel A.J.E. (2003) The phloem, a miracle of ingenuity. *Plant, Cell & Environment* **26**, 125–149.
- Wanek W., Heintel S. & Richter A. (2001) Preparation of starch and other carbon fractions from higher plant leaves for stable carbon isotope analysis. *Rapid Communications in Mass Spectrometry* **15**, 1136–1140.
- Werner C., Unger S., Pereira J.S., Rodrigo M., David T.S., Kurz-Beson C., David J.S. & Maguas C. (2006) Importance of short-term dynamics in carbon isotope ratios of ecosystem respiration ( $\delta^{13}\text{C}$ ) in a Mediterranean oak woodland and linkage to environmental factors. *New Phytologist* **172**, 330–346.
- Yakir D. & Wang X.F. (1996) Fluxes of CO<sub>2</sub> and water between terrestrial vegetation and the atmosphere estimated from isotope measurements. *Nature* **380**, 515–517.

Received 28 February 2008; accepted for publication 3 March 2008